Effect of band nonparabolicity on mobility in a δ-doped semiconductor

L. R. González
Departamento de Física, Facultad de Ciencias, Universidad de Los Andes, Mérida 5101, Venezuela

J. Krupski
Instytut Fizyki Teoretycznej, Uniwersytet Warszawski, ul. Hoża 69, PL-00-681 Warszawa, Poland and Instytut Fizyki, Uniwersytet w Białymstoku, ul. Lipowa 41, PL-15-424 Białystok, Poland

M. Pietka
Instytut Fizyki, Uniwersytet w Białymstoku, ul. Lipowa 41, PL-15-424 Białystok, Poland

T. Szwacka
Departamento de Física, Facultad de Ciencias, Universidad de Los Andes, Mérida 5101, Venezuela
(Received 5 November 1998)

We calculate the low-temperature mobility of a two-dimensional (2D) electron gas in δ-doped GaAs by solving coupled Boltzmann equations in the relaxation-time approximation using one-, two-, or three-subband models depending on the population of the subbands. We assume that the mobility is limited by ionized impurity scattering, including intersubband contribution. Our results suggest that the nonparabolicity of the conduction band plays the important role: it reduces the calculated 2D electron-gas mobility by about 20%, which leads to a better agreement with experimental data. [S0163-1829(99)17035-8]

I. INTRODUCTION

During the last several years, δ-doped semiconductors have received considerable attention due to their fundamental and technological aspects (see the reviews in Ref. 1). In our earlier papers,[2,3] we calculated low-temperature, two-dimensional electron-gas (2DEG) mobility in δ-doped GaAs assuming that the electrons are scattered from ionized donors which are localized in a single atomic layer[2] or are spread out at uniform density over some distance.[3] In the second case the broadening of the doping profile resulted in the reduction of the mobility, however, the calculated mobilities were still about several dozen percent higher than the measured ones.

In the present paper we examine the influence of conduction-band nonparabolicity on 2DEG mobility in a δ-doped semiconductor. We are concerned with δ Si-doped GaAs with nonvanishing background acceptor density. We limit ourselves to the low-temperature case, assuming that the electrons are scattered by the ionized impurities only. To determine the mobility we solve coupled Boltzmann equations in the relaxation-time approximation using one-, two-, or three-subband models depending on the subband population.

II. SUBBAND STRUCTURE FOR A δ-DOPED SEMICONDUCTOR

We consider a weakly *p*-type GaAs with a highly doped n^+ layer of finite thickness with all donors (e.g., Si atoms) ionized. We assume that the positive charge is uniformly distributed in a thin layer ($-d_0 \leqslant z \leqslant d_0$). This configuration is illustrated schematically in Fig. 1.

For simplicity, the effective-mass Hamiltonian is taken to be (see, for example, Refs. 4 and 5)

$$H = \alpha_1 \nabla^4 - \alpha_2 \nabla^2 + V. \tag{1}$$

The corrections due to conduction-band nonparabolicity are represented by the $\alpha_1 \nabla^4$ term only, i.e., the band warping is neglected,

$$\alpha_1 = \frac{\hbar^4}{4E_g}\left(\frac{1}{m} - \frac{1}{m_0}\right)^2, \quad \alpha_2 = \frac{\hbar^2}{2m}, \tag{2}$$

and $V = V(z)$ is the confinement potential that includes electron-electron interaction. The eigenfunctions and eigenvalues of Eq. (1) can be sought in the forms

$$\psi_{n\vec{k}}(\vec{r}) = \frac{1}{2\pi}\exp(i\vec{k}\vec{\rho})h_{nk}(z), \tag{3}$$

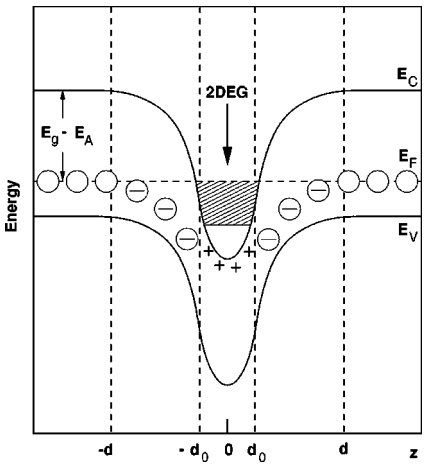

FIG. 1. Schematic behavior of the potential $V(z)$ experienced by electrons in a δ-doped semiconductor with a nonvanishing acceptor density and a finite ($2d_0$) width of the donor distribution.

$$E_{nk}=E(n,k)+\alpha_2 k^2-\alpha_1 k^4, \tag{4}$$

where $\vec{\rho}=(x,y)$ and $\vec{k}=(k_x,k_y)$. Both h_{nk} and $E(n,k)$ satisfy one-dimensional Schrödinger equation

$$\left[-\alpha_1\frac{\partial^4}{\partial z^4}+2\alpha_1 k^2\frac{\partial^2}{\partial z^2}-\alpha_2\frac{\partial^2}{\partial z^2}+V(z)\right]h_{nk}(z)$$
$$=E(n,k)h_{nk}(z). \tag{5}$$

To find $V(z)$, we employ the Thomas-Fermi approximation which is already accurate to better than a few percent as compared with the more realistic but at the same time more laborious self-consistent method.[6] Classical expression for the Fermi energy E_F used in the Thomas-Fermi approximation (see, for example, Ref. 7, Chap. 1 Sec. 9) here takes the form

$$E_F=\alpha_2 k_{\mathrm{F}}^2(\vec{r})+\alpha_1 k_{\mathrm{F}}^4(\vec{r})+V(\vec{r}). \tag{6}$$

Now the Poisson equation reads (the energy is measured from the Fermi level E_F)

$$\frac{d^2V}{dz^2}=-\frac{4}{3\pi}\frac{e^2}{\epsilon_0}\left(\frac{2m}{\hbar^2}\right)^{3/2}[-V(z)]^{3/2}\left[1-\frac{3}{2}\frac{V(z)}{E_g'}\right]$$
$$+4\pi\frac{e^2}{\epsilon_0}n_D(z)-4\pi\frac{e^2}{\epsilon_0}n_A(z), \tag{7}$$

where n_D and n_A are the ionized donor and acceptor 3D density, respectively. The first term on the right-hand side is the electron charge density obtained in the Thomas-Fermi approximation. The expression $-3V/2E_g'$ is the first-order correction due to the nonparabolicity, and $E_g'=E_g(1-m/m_0)^{-2}$.

To calculate $E(n,k)$ we apply the perturbation theory to Eq. (5), treating $-\alpha_1\partial^4/\partial z^4+2\alpha_1 k^2\partial^2/\partial z^2$ as a perturbation. Solutions to the unperturbed problem $E^0(n,k)=E_n-\alpha_2 k^2+\alpha_1 k^4$ and h_{nk}^0 were obtained numerically. Finally,

$$E_{nk}=[E^0(n,k)+E^1(n,k)+\cdots]+\alpha_2 k^2-\alpha_1 k^4$$
$$\simeq\tilde{E}_n+\alpha_2(n)k^2-\alpha_1 k^4, \tag{8}$$

where $\tilde{E}_n=E_n^0-\alpha_1\int dz|\partial^2 h_n^0/\partial z^2|^2$ and $\alpha_2(n)=\alpha_2-2\alpha_1\int dz|\partial h_n^0/\partial z|^2$.

Now the transport mass $m_n=\hbar^2 k(dE_{nk}/dk)^{-1}$ depends on both energy E and the subband index n:

$$m_n(E)=\frac{\hbar^2}{2\alpha_2(n)}\left[1-\frac{4\alpha_1}{\alpha_2^2(n)}(E-\tilde{E}_n)\right]^{-1/2}. \tag{9}$$

The density of states function $D(E)$ reads

$$D(E)=\sum_n\frac{m_n(E)}{\pi\hbar^2}\theta(E-\tilde{E}_n), \tag{10}$$

and, what follows, the concentration of 2DEG in the sth subband at $T=0$ K is

$$n_s(E_F)=\frac{\alpha_2(s)}{4\pi\alpha_1}\left\{1-\left[1-\frac{4\alpha_1}{\alpha_2^2(s)}(E_F-\tilde{E}_s)\right]^{1/2}\right\}. \tag{11}$$

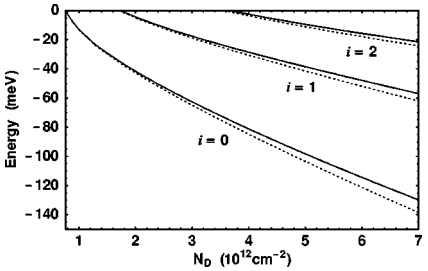

FIG. 2. Subband separation E_i-E_F in δ-doped GaAs with a background acceptor concentration $n_A=5\times10^{15}$ cm^{-3} vs areal donor concentration N_D. The width $2d_0$ of the square-shaped donor distribution is 50 Å. The solid and dashed lines are for nonparabolic and parabolic conduction bands, respectively.

Note that both formulas (10) and (11) reduce to a familiar form when nonparabolicity is neglected, i.e., $\alpha_1=0$.

The influence of nonparabolicity on subband structure is illustrated in Fig. 2. It turns out that the subband bottoms are shifted by the nonparabolicity to higher energies. At the same time the nonparabolicity leads to a lowering of 2DEG concentrations n_i in individual subbands for $i>0$, as shown in Fig. 3. In contrast to it, the electron concentration n_0 in the lowest subband is higher than that calculated within the parabolic approximation. This agrees with the results of Zrenner, Koch, and Ploog,[8] who used a more realistic formula for the conduction-band dispersion.

III. MOBILITY LIMITED BY IONIZED IMPURITY SCATTERING

The system we deal with is δ Si-doped GaAs, with a nonvanishing acceptor background density n_A. We restrict ourselves to the $T=0$ case, and calculate the mobility limited by the scattering from ionized donors which are uniformly distributed within $2d_0$. The scattering from acceptors can be ignored.

Both the transport and Hall mobilities can be calculated in the usual way.[9,10] It turns out that the nonparabolic band formulas can be obtained from the parabolic band ones by the replacement of m by $m_n(E_F)$ [Eq. (9)] and $n_s(E_F)=m(E_F-E_s)/\pi\hbar^2$ by $n_s(E_F)$ given by Eq. (11). The low-temperature transport mobility μ and the Hall mobility μ_H are given by

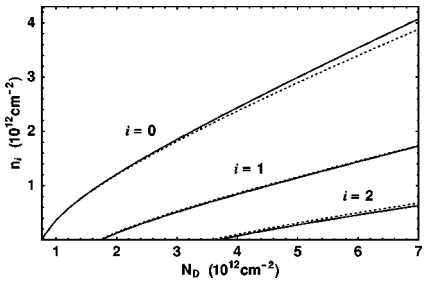

FIG. 3. 2DEG concentrations n_i in the individual subbands vs areal donor concentration N_D in δ-doped GaAs for the same case as in Fig. 2.

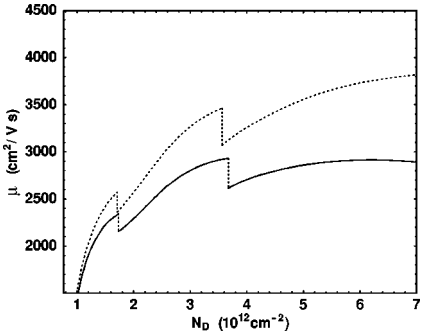

FIG. 4. Calculated transport mobilities of the 2DEG in δ-doped GaAs for the same case as in Fig. 2.

$$\mu=\frac{\sum_i n_i(E_F)\mu_i(E_F)}{\sum_j n_j(E_F)}, \quad \mu_H=\frac{\sum_i n_i(E_F)\mu_i^2(E_F)}{\sum_j n_j(E_F)\mu_j(E_F)}, \tag{12}$$

where

$$\mu_i(E)=\frac{|e|}{m_i(E)}\tau_i(E) \tag{13}$$

is the mobility in the ith subband. Relaxation times τ_i satisfy coupled linear equations

$$P_n(E)\tau_n(E)-\sum_{n'\neq n} P_{nn'}(E)\tau_{n'}(E)=1, \tag{14}$$

where $P_n(E)$ and $P_{nn'}(E)$ are $(E>\tilde{E}_n)$

$$P_n(E)=\frac{n_D}{2\pi\hbar^3}m_n(E)\int_{-d_0}^{d_0}dz\int_0^{2\pi}d\phi|V_{\mathrm{eff}_{nn}}(q,z)|^2 \times(1-\cos\phi)+\frac{n_D}{2\pi\hbar^3}\sum_{n'\neq n}m_{n'}(E)\int_{-d_0}^{d_0}dz \times\int_0^{2\pi}d\phi|V_{\mathrm{eff}_{nn'}}(q',z)|^2\theta(E-\tilde{E}_{n'}), \tag{15}$$

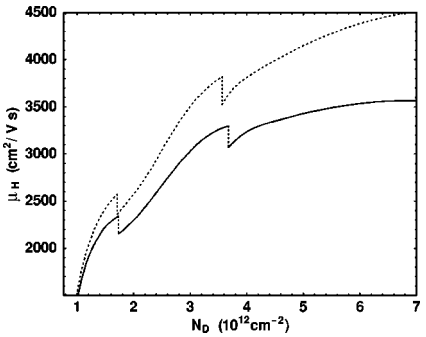

FIG. 5. Calculated Hall mobilities of the 2DEG in δ-doped GaAs for the same case as in Fig. 2.

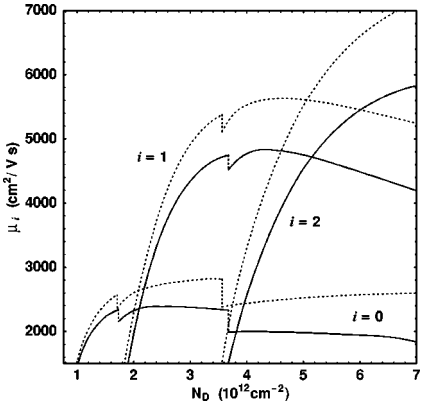

FIG. 6. Calculated subband mobilities μ_i in δ-doped GaAs for the same case as in Fig. 2.

$$P_{nn'}(E)=\frac{n_D}{2\pi\hbar^3}m_n(E)\left[\frac{n_{n'}(E)}{n_n(E)}\right]^{1/2} \times\int_{-d_0}^{d_0}dz\int_0^{2\pi}d\phi|V_{\mathrm{eff}_{nn'}}(q',z)|^2\cos\phi. \tag{16}$$

Here $q=k[2(1-\cos\phi)]^{1/2}$ and $q'=(k^2+k'^2-2kk'\cos\phi)^{1/2}$, where $k^2=2\pi n_n(E)$ and $k'^2=2\pi n_{n'}(E)$. Matrix elements of the effective potential V_{eff} experienced by electrons are related to the matrix elements of the impurity potential V_{imp} (here ionized donors) by

$$V_{\mathrm{eff}_{nn'}}(\vec{q},z)=\sum_{ll'}\epsilon^{-1}_{nn',ll'}(\vec{q})V_{\mathrm{imp}_{ll'}}(\vec{q},z), \tag{17}$$

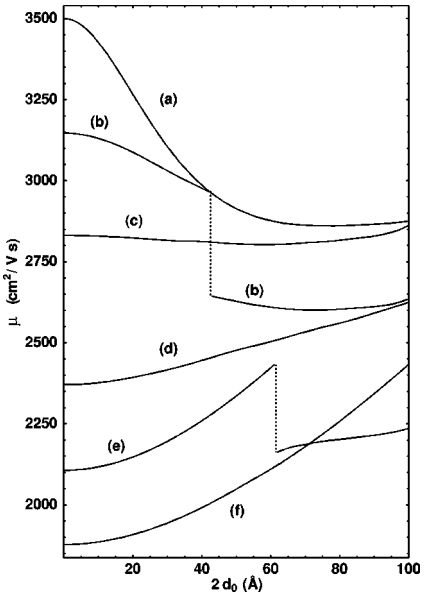

FIG. 7. Calculated transport mobilities of the 2DEG in δ-doped GaAs vs the width $2d_0$ of the square-shaped donor distribution for a nonparabolic band. Areal donor concentrations N_D: curve *a*, 6×10^{12} cm^{-2}; curve *b*, 3.7×10^{12} cm^{-2}; curve *c*, 3×10^{12} cm^{-2}; curve *d*, 2.3×10^{12} cm^{-2}; curve *e*, 1.7×10^{12} cm^{-2}; curve *f*, 1.3×10^{12} cm^{-2}. The background acceptor concentration is $n_A=5\times10^{15}$ cm^{-3}.

with ϵ^{-1} being an inverse dielectric matrix. In our notation $V_{nn'}(\vec{q},z)$ are the 2D Fourier transforms $[\vec{q}=(q_x,q_y)]$,

$$V_{nn'}(\vec{q},z)=\int d^2\rho V_{nn'}(\vec{\rho},z)\exp(-i\vec{q}\vec{\rho}) \tag{18}$$

of the matrix elements with respect to ρ of the potential $V(\vec{\rho},z)$ in three dimensions:

$$V_{nn'}(\vec{\rho},z)=\int dz' h_n^*(z')V(\vec{\rho},z-z')h_{n'}(z'). \tag{19}$$

In numerical calculations, we use the dielectric matrix obtained in the random-phase approximation (Ref. 10; see also Ref. 2 for details). In our calculations nonparabolic corrections to the screening are ignored.

Low-temperature mobilities limited by the Coulomb scattering are calculated numerically from formulas (12)–(19) and plotted as functions of areal donor concentration $N_D=2d_0n_D$ in Figs. 4 (transport mobility), 5 (Hall mobility), and 6 (subband mobilities) for the doping layer width $2d_0=50$ Å (realistic δ doping in contrast to genuine δ doping when $d_0\rightarrow 0$). These results are compared with those for the parabolic band. Figure 7 shows how the transport mobilities depend on doping layer thickness.

We checked numerically that $m(E)$ dependence accounts for most of the change in the electron mobility due to the nonparabolicity of the conduction band. Nonparabolic corrections to $n_s(E)$ as well as to the subband structure can be ignored in the first step when determining μ. The error of such an approximation does not exceed several percent.

IV. CONCLUSIONS

Our results suggest that one would have to take band nonparabolicity into account to achieve better agreement between theory and experiment. The mobilities calculated according to Eqs. (12)–(19) are now close to the experimental values, and we believe they are accurate within about 20% (calculated mobilities are higher than the measured ones). Note that the significant scatter among the measured mobilities (see, for example, Ref. 1, Chap. 17, and references therein), which can be attributed to uncertainties in the specification of sample parameters, makes any detailed comparison of the results rather difficult.

In our previous paper[3] we discussed the possibility to observe discontinuities in the low-temperature 2DEG mobility in a δ-doped semiconductor at $E_F=E_n$. Here we would like to point out only that the nonparabolicity effect does not change the conclusion of that discussion. 2DEG mobility exhibits drops as a function of the width of the doping profile (see Fig. 7). The thickness of the doping profile in a given sample can be changed with the help of annealing.[11–14] As in the previous case (Fig. 5 in Ref. 3), the drops mentioned above are about four times larger than the error in most precise experiments. Note, however, that the discontinuities in the 2DEG mobility can be smeared out due to the level broadening, which should be taken into account in more realistic calculations.

ACKNOWLEDGMENTS

This work was partially supported by the Consejo de Desarollo Científico Humanístico y Technológico de la Universidad de Los Andes, Mérida, Venezuela.

[1] *Delta-doping of Semiconductors*, edited by E. F. Schubert (Cambridge University Press, London, 1996).
[2] L. R. González, J. Krupski, and T. Szwacka, Phys. Rev. B **49**, 11 111 (1994). Note that part of Figs. 3 and 4 in this paper are incorrect; however, the errors do not change the conclusions. The correct presentation is given in **52**, 11 518(E) (1995).
[3] L. R. González, J. Krupski, and T. Szwacka, Phys. Rev. B **54**, 7658 (1996).
[4] D. F. Nelson, R. C. Miller, and D. A. Kleinman, Phys. Rev. B **35**, 7770 (1987).
[5] A. Persson and R. M. Cohen, Phys. Rev. B **38**, 5568 (1988).
[6] J. Krupski and M. Pietka, Solid State Commun. **107**, 141 (1998).
[7] N. H. March, W. H. Young, and S. Sampanthar, *The Many-Body Problem in Quantum Mechanics* (Cambridge University Press, Cambridge, 1967).
[8] A. Zrenner, F. Koch, and K. Ploog, Surf. Sci. **196**, 671 (1988).
[9] E. D. Siggia and P. C. Kwok, Phys. Rev. B **2**, 1024 (1970).
[10] S. Mori and T. Ando, Phys. Rev. B **19**, 6433 (1979).
[11] P. M. Koenraad, A. C. L. Heessels, F. A. P. Blom, J. A. A. J. Perenboom, and J. H. Wolter, Physica B **184**, 221 (1993).
[12] P. M. Koenraad, I. Barsony, A. F. W. van der Stadt, J. A. A. J. Perenboom, and J. H. Wolter, in *International Conference on Defects in Semiconductors, Gmunden, Austria, 1993*, Materials Science Forum Vols. 143–147 (Trans Tech, Aedermannsdorf, Switzerland, 1994), p. 663.
[13] E. F. Schubert, J. B. Stark, B. Ullrich, and J. E. Cunningham, Appl. Phys. Lett. **52**, 1508 (1988).
[14] E. F. Schubert, J. B. Stark, T. H. Chiu, and B. Tell, Appl. Phys. Lett. **53**, 293 (1988).